Supplementary Information for "Ad Aurum: Tunable Transfer of N-heterocyclic Carbene Complexes to Gold Surfaces"

Nathaniel L. Dominique,[a] Ran Chen,[b] Alyssa V. B. Santos,[b] Shelby L. Strausser,[c] Theodore Rauch,[a] Chandler Q. Kotseos,[a] William C. Boggess,[a] Lasse Jensen,[b*] David M. Jenkins,[c*] and Jon P. Camden[a*]

a. Department of Chemistry and Biochemistry, University of Notre Dame, Notre Dame, Indiana 46556, United States

b. Department of Chemistry, 101 Chemistry Building, Penn State University, University Park, PA 16802

c. Department of Chemistry, University of Tennessee, Knoxville, Knoxville, Tennessee 37996, United States

Table of Contents

Table of Figures

Materials and Methods

Materials

Chloro[1,3-dihydro-1,3-bis(1-methylethyl)-2H-benzimidazol-2-ylidene] gold(I) was purchased from STREM chemicals (>95%, CAS# 953820-59-2, product # 79-1250). Chloro[1,3-bis(2,6-diisopropylphenyl)imidazol-2-ylidene] gold(I), silver(I) and copper(I) carbene complexes were acquired from Sigma Aldrich with CAS numbers of 852445-83-1, 873297-19-9 and 578743-87-0, respectively. Reagent alcohol was purchased from VWR. Ultrapure water was generated in house using a Thermo Scientific Barnstead system and was filtered until the resistivity exceeded 18 Megaohms. ACS Reagent grade Gold(III) trichloride trihydrate and trisodium citrate trihydrate were purchased from Sigma Aldrich. All chemicals were used as received. [1,3-di-isopropyl-benzimidazol-2-ylidene]AgBr was synthesized according to the method of Ghosh. [1] 25 x 25 mm ITO coated glass substrates used for x-ray photoelectron analysis were obtained from Ossila.

Gold nanoparticle (AuNP) synthesis

All glassware for the AuNP synthesis was cleaned with *aqua regia* (3:1 concentrated hydrochloric acid to nitric acid). *Aqua regia* is extremely dangerous and should only be used with the proper safety precautions in place. Synthesis of gold nanoparticles (AuNPs) was performed according to the Lee and Meisel method. [2] Briefly, 240 mg of gold(III) trichloride trihydrate dissolved in 500 mL ultrapure water (18 MΩ) was brought to a boil while stirring vigorously. 50 mL of 1% sodium citrate tribasic was added all at once and the resulting wine-red solution was boiled for 45 minutes with vigorous stirring. The colloidal suspension was diluted to 1000 mL and kept in an amber glass bottle. The colloids were analyzed using scanning electron microscopy (SEM), UV-Vis, and DLS techniques.

Treatment of AuNPs with carbene complexes

For nanoparticles functionalized with ligand **1**, 74.4 µL of a one mM carbene stock solution in acetonitrile was added to five mL of AuNPs and vortexed for approximately 30 minutes resulting in a ligand loading of 14.9 µM. All carbene functionalized gold nanoparticles self-aggregated at this concentration.

For nanoparticles functionalized with ligand **2**, five µL of a ten mM carbene stock solution in acetonitrile was added to five mL of AuNPs and vortexed for approximately 30 minutes resulting in a ligand loading of ten µM. Only AuNPs treated with (**2**)CuCl self-aggregated at this concentration, whereas AuNPs treated with (**2**)AuCl or (**2**)AgCl did not self-aggregate.

Theoretical Calculations

Each carbene molecule was bound to a gold cluster with a gold, silver, or copper adatom in the simulated model systems. All calculations in this work were performed using a local version of the Amsterdam density functional (ADF) program package. [3, 4] The Becke–Perdew (BP86) XC-potential [5, 6] with dispersion correction Grimme3 BJDAMP [7]was used. The triple-ζ polarized slater type (TZP) basis set with small frozen cores from the ADF basis set library was used. The scalar relativistic effects were accounted for by the zeroth-order regular approximation (ZORA). [8] For the systems in this work, constraint geometry optimization was performed, where only the carbene molecule and the adatom were relaxed. Accordingly mobile block hessian frequency calculations were performed. [9, 10] Polarizability calculations were performed using the AOResponse module with the Adiabatic Local Density Approximation (ALDA). [11] The polarizability derivatives were calculated by numerical differentiation with respect to the normal mode displacements. For any system in this work, the molecule–cluster axis was aligned with the z-axis and only the zz components in the polarizabilities were considered. The structure diagrams of the model systems in this work, were plotted using PyMOL. [12]

LDI-MS characterization

One Bruker UltrafleXtreme MALDI-TOF-TOF instrument equipped with a frequency tripled ND:YAG laser (355 nm excitation) and a 384 spot Bruker polished steel sample target was employed for all experiments. All spectra were acquired using positive ion mode scans where the reflector was set to positive mode and data collected from 60-10,000 Daltons. The max laser power is expressed as a percentage of highest achievable power with a global attenuator offset of 48%. In general, at least 2000 laser shots per spectra with 50% of the max laser power was used for NHC-AuNPs, unless otherwise noted.

The UltrafleXtreme instrument was calibrated using a peptide mixture of Bradykinin(1-7) (757.39916 m/z), Angiotensin (1046.54180 m/z and 1296.68480 m/z), Substance P (1347.73540 m/z), Bombesin[M+H] (1619.82230 m/z), Renin (1758.93261 m/z), ACTH (2093.08620 m/z and 2465.19830 m/z), and Somatostatin (3147.47100 m/z).

For AuNP samples functionalized with (**1**)AuCl or (**1**)AgBr, approximately 4 mL of the 5 mL total volume was removed carefully without disturbing the aggregated nanoparticles. An equivalent amount of water was added, the vial shaken gently, the particles allowed to settle, and finally ~4 mL of supernatant was removed. This process was repeated once more with ultrapure water and once

with reagent alcohol. Then one 1.5 µL aliquot of the freshly sonicated nanoparticle suspension was drop-cast onto the sample target plate and analyzed with LDI-MS.

For AuNP samples functionalized with (**2**)AuCl or (**2**)AgCl, the nanoparticles were washed by centrifuging the particles at 10K RPM, removing 0.9 mL of supernatant without disturbing the aggregated particles, sonicating, and then adding 0.9 mL of ultrapure water. After another round of centrifugation at 9k RPM, 0.9 mL of supernatant was removed, the particles sonicated, and 0.9 mL of reagent alcohol was added. The particles were then centrifuged at 8k RPM before removing as much supernatant as possible without disturbing the nanoparticles. 0.2 mL of ultrapure water was added, the sample sonicated, and then transferred to a glass vial.

For AuNPs treated with (**2**)CuCl, the nanoparticles were washed according to the same method used for self-aggregated nanoparticles treated with NHC complexes of **1**.

LDI-MS data was converted to MzML files using the Bruker compassXport command line utility, read into python using OpenMS software, [13] and baseline subtracted using the Zhang algorithm. [14]

X-ray photoelectron spectroscopy

XPS measurements were obtained with a PHI VersaProbe II surface analysis instrument (Physical Electronics) equipped with monochromatic Al Kα X-ray source (photon energy = 1486.6 eV). High-resolution spectra were obtained for at least two sample spots using a 23.50 eV pass energy under ultrahigh vacuum conditions. All resulting spectra were summed together and calibrated versus the binding energy of Au 4f peak at 84.0 eV. [15] The spectra were then background-subtracted using a Shirley algorithm[16] generated using python code from LG4X open source software. [17] Peak locations for high resolution scans were determined using the lmfit module[18] in Python 3.9 with a VoigtModel. [16] XPS data was analyzed using the *Handbook of X-ray Photoelectron Spectroscopy*[19] and the NIST database for XPS spectroscopy.

Samples were mounted for XPS by drop-casting 1.5 µL of washed gold nanoparticles (see LDI-MS sample prep for washing procedure) onto an ITO coated glass slide 25 x 25 millimeters (Ossila). The glass slide was mounted onto a target plate using conductive copper tape to ground the sample. The samples were dried under rough vacuum for two hours prior to analysis.

SERS characterization

Surface-enhanced Raman spectroscopy (SERS) was carried out using a home-built set-up. A 633 nm HeNe laser (Thorlabs) was directed into an inverted microscope (Nikon Ti-U) and focused onto the aggregated gold nanoparticles with an objective lens (20×, NA = 0.5). Scattered light was collected through the same objective, filtered through a Rayleigh rejection filter (Semrock), and fed into a spectrometer (Princeton Instruments Action SP2300, f = 0.3 mm, 1200 $g \cdot mm^{-1}$). Spectra were analyzed using Winspec32 software (Princeton Instruments).

SERS data was read into python using python NumPy and baseline subtracted using the Zhang algorithm. [14] The spectra shown are the average of at least five measurements of washed (see LDI-MS sample prep for washing procedure) gold nanoparticles which all self-aggregated after successive washing steps.

UV-Vis characterization

A VWR UV-3100 Spectrophotometer equipped with D_2 and tungsten lamps was employed along with a one cm plastic cuvette to collect all spectra of the AuNP solutions. Ultrapure water (18 MΩ) was used as a blank.

High Resolution Mass Spectrometry

High resolution mass spectrometry measurements were acquired on a Bruker Impact II instrument of (**2**)AuCl (10 µM in acetonitrile) to confirm the mass assignments observed in LDI-MS.

Inductively Coupled Plasma Optical Emission Spectroscopy (ICP-OES)

ICP-OES analysis was performed on a Perkin Elmer Optima 8000 instrument equipped with a Prep 3 autosampler. Calibration curves were prepared using Au, Ag, and Cu atomic absorption standards (Thermo Fisher) with concentrations of 980 ± 5 µg/g, 999 ± 4 µg/g,

and 1002 ± 6 µg/g, respectively. Calibrants used in ICP-OES analysis of AuNPs treated with (**1**)AuCl and (**1**)AgBr were prepared at the following concentrations using gravimetric methods:

Au Calibrants: 74.999, 50.057, 25.156, 9.997, 0.998, and 0.504 µg/g in 5% aqua regia

Ag calibrants: 5.138, 1.035, 0.505, 0.100, 0.052, and 0.010 µg/g in 5% nitric acid

Calibrants used in ICP-OES analysis of AuNPs treated with (**2**)AuCl, (**2**)AgCl, or (**2**)CuCl were prepared at the following concentrations using gravimetric methods:

Au Calibrants: 74.999, 50.057, 25.156, 9.997, 0.998, and 0.504 µg/g in 5% aqua regia

Ag calibrants: 5.055, 1.040, 0.519, 0.105, 0.052, and 0.011 µg/g in 5% nitric acid

Cu calibrants: 5.065, 1.053, 0.523, 0.104, 0.053, and 0.012 µg/g in 5% nitric acid

Gold nanoparticles treated with (**1**)AuCl, (**1**)AgBr, (**2**)AuCl, (**2**)AgCl, or (**2**)CuCl were washed (vide supra), dried on a hot-plate, and digested in 0.5 mL aqua regia for at least 30 minutes. Then 9.5 mL of 18 MΩ water was added. The experimental yield of silver or copper in the AuNPs treated with Ag or Cu NHC complexes is expressed as the ppm concentration of Ag or Cu divided by the ppm concentration of Au in the solution. The theoretical yield is expressed as the mass of Ag or Cu from the NHC complexes over the mass of Au in 5 mL of colloids. The percent of Ag or Cu incorporation is expressed as the experimental yield divided by the theoretical yield.

The error associated with the calibration curves was estimated according to the method of Harris[20] and used to estimate the error of calculated concentrations and percent Ag or Cu alloying with Au. The LINEST Function in Microsoft Excel was used to calculate the slope and intercept, error of slope and intercept, and the R^2 value. Signal intensities were corrected during data acquisition using the Perkin Elmer software.

Nanoparticle characterization

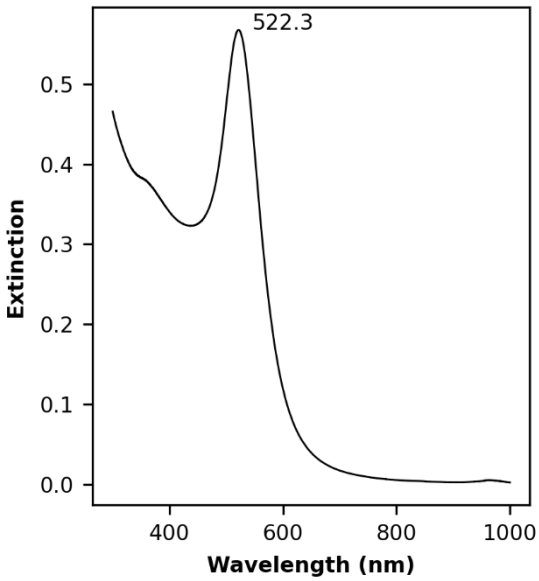

Figure S1. Extinction spectrum of gold colloids synthesized according to the Lee and Meisel Method. The AuNPs were diluted by a factor of 4 in ultrapure water.

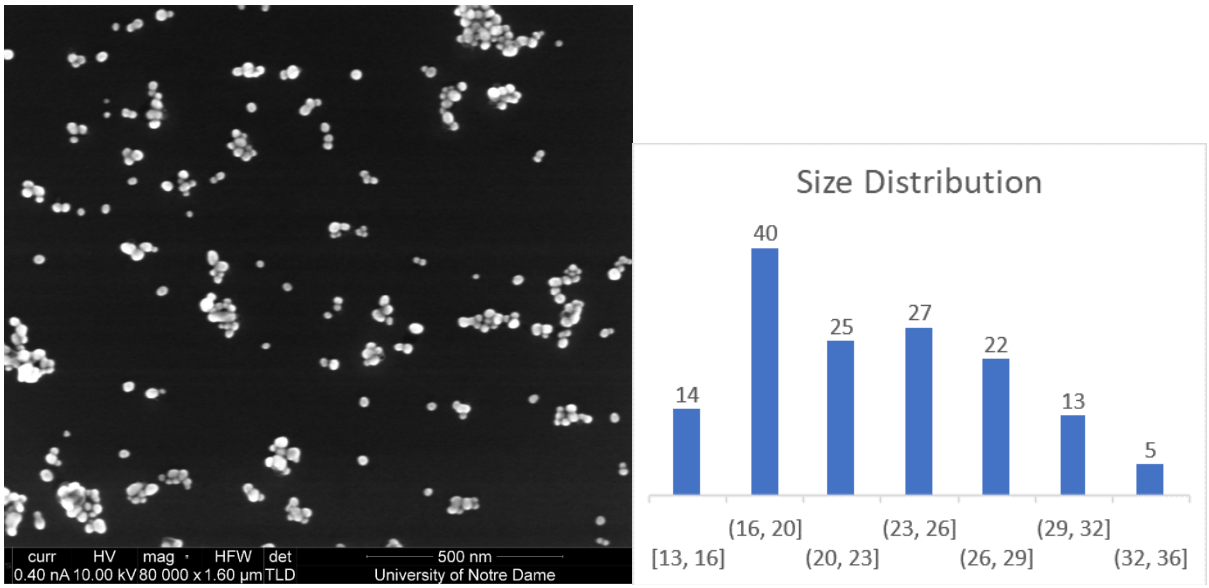

Figure S2. Field emission scanning electron microscopy image of 23 ± 5 nm AuNPs with uncertainties represented using the standard deviation.

Table S1. DLS analysis of citrate-capped AuNPs synthesized according to the Lee and Meisel method illustrating a diameter of approximately 22 nm.

Type	Sample ID	Eff. Diam. (nm)	Polydispersity	Count Rate (kcps)	Diffusion Coeff. (cm²/s)
DLS	Sample 1	21.74	0.332	433.1	2.257E-07
DLS	Sample 2	21.97	0.320	435.7	2.234E-07
DLS	Sample 3	21.56	0.333	434.6	2.276E-07
	Mean:	21.76	0.329	434.5	2.256E-07
	Std Err:	0.12	0.004	0.8	1.223E-09
	Std Dev:	0.20	0.007	1.3	2.118E-09

SERS of AuNPs treated with (1)AuCl and (1)AgBr

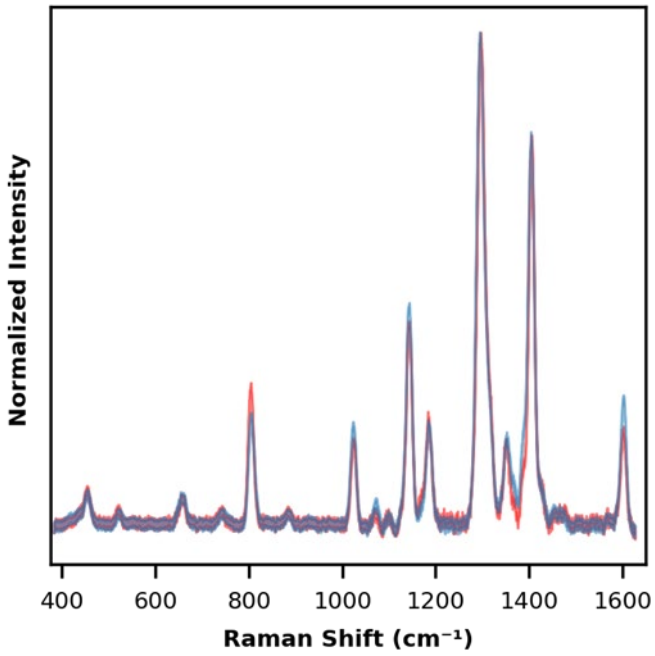

Figure S3. SERS spectra of AuNPs mixed with (**1**)AuCl (red) or (**1**)AgBr (blue) expressed using the bounds of a 95% confidence interval calculated using six replicate measurements.

Table S2. Peak locations from SERS spectra (Figure 4, main text) of AuNPs treated with (**1**)AuCl or (**1**)AgBr. Peak positions were determined using the lmfit module to fit a Lorentzian peak shape to each major peak in the spectra. These data illustrate that no significant peak shift occurs for each system.

AgNHC	**AuNHC**	**Difference**
ω (cm^{-1})	ω (cm^{-1})	ω (cm^{-1})
1601.7	1601.4	0.4
1474.0	1476.9	-3.0
1463.1	1464.0	-0.9
1404.0	1406.4	-2.4
1352.6	1351.0	1.6
1302.2	1304.4	-2.2
1292.5	1295.1	-2.6
1185.1	1184.3	0.8
1142.6	1143.1	-0.5
1098.1	1098.2	-0.1
1071.8	1068.5	3.3
1023.2	1022.9	0.3
884.1	884.0	0.1
804.8	803.9	1.0

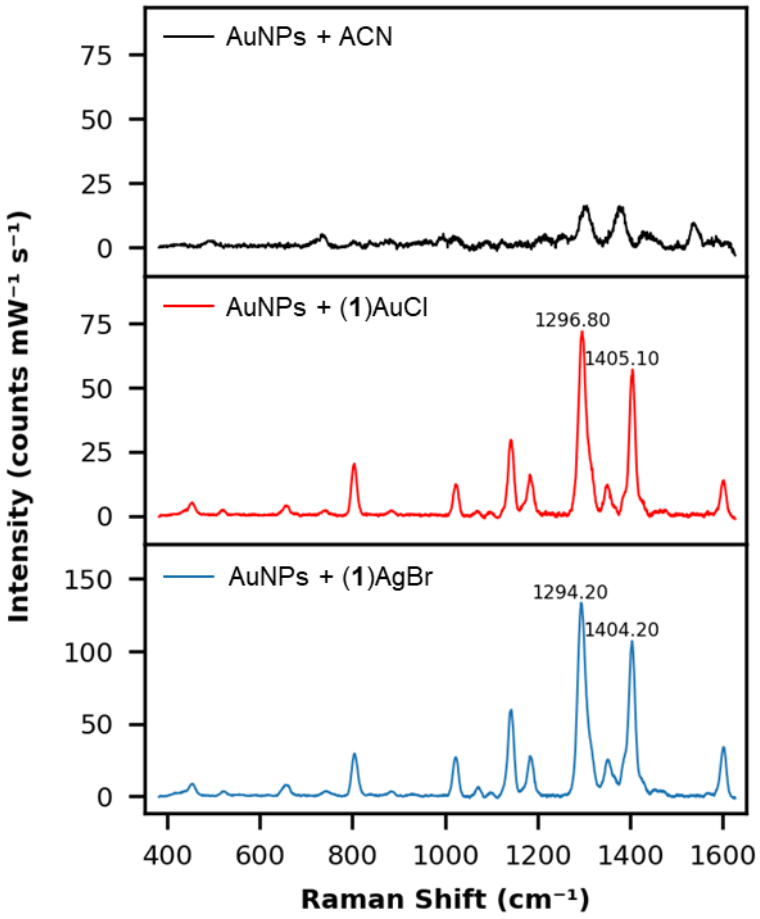

Figure S4. SERS spectra of AuNPs treated with acetonitrile solvent as a control (top), (**1**)AuCl (middle), and (**1**)AgBr (bottom) illustrate the rich vibrational signatures of the NHC systems not present in the AuNP control.

SERS of AuNPs treated with (2)AuCl, (2)AgCl and (2)CuCl

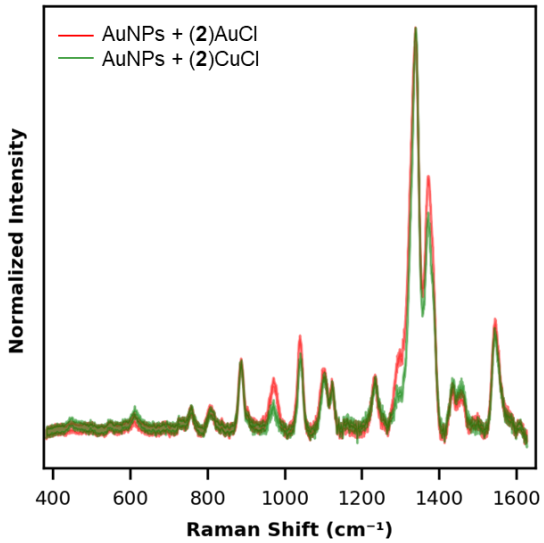

Figure S5. SERS spectra of AuNPs mixed with (**2**)AuCl (red) or (**2**)CuCl (green) expressed using the bounds of a 95% confidence interval calculated using five replicate measurements.

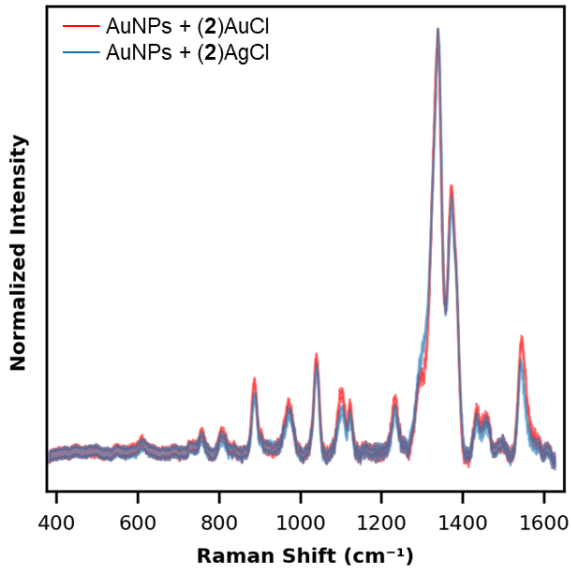

Figure S6. SERS spectra of AuNPs mixed with (**2**)AuCl (red) or (**2**)AgCl (blue) expressed using the bounds of a 95% confidence interval calculated using five replicate measurements.

Exact Mass Measurements of (2)AuCl

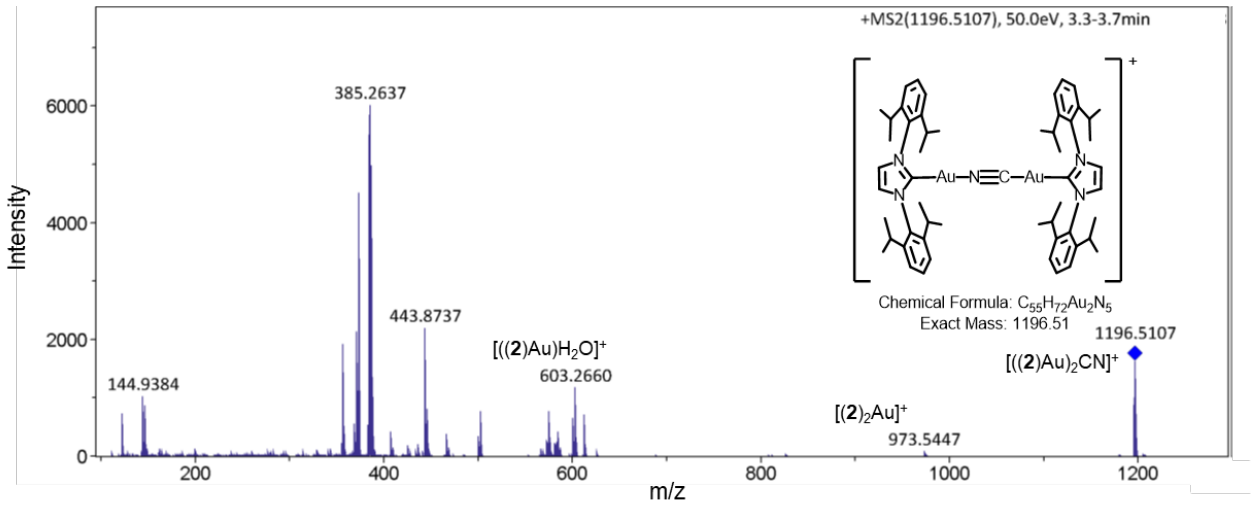

Figure S7. +MS2 spectra of (**2**)AuCl illustrating formation of $[((\mathbf{2})Au)_2CN]^+$ ions at 1196.5107 (ppm of 0.99). These data provide corroborating evidence for our assignment of the peak observed in LDI-MS at 1196 as $[((\mathbf{2})Au)_2CN]^+$ ions.

XPS survey scans

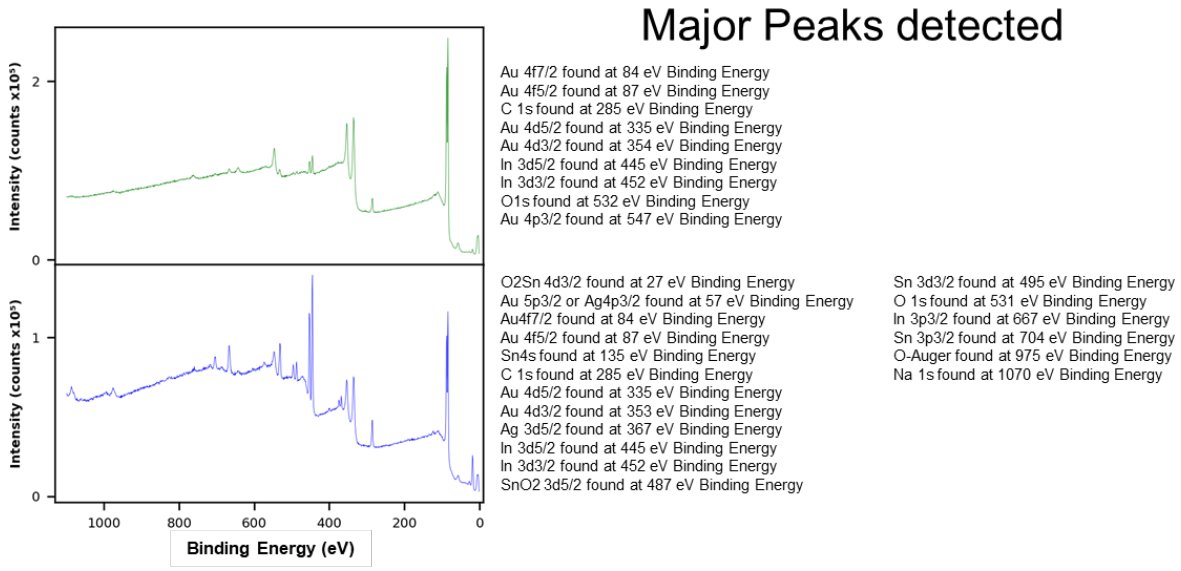

Figure S8. XPS survey scan of AuNPs treated with (**1**)AuCl (top) or (**1**)AgBr (bottom) . The spectra illustrate that the ITO substrate is not completely covered by the AuNPs since some peaks corresponding to indium oxide or tin oxide appear in each spectrum.

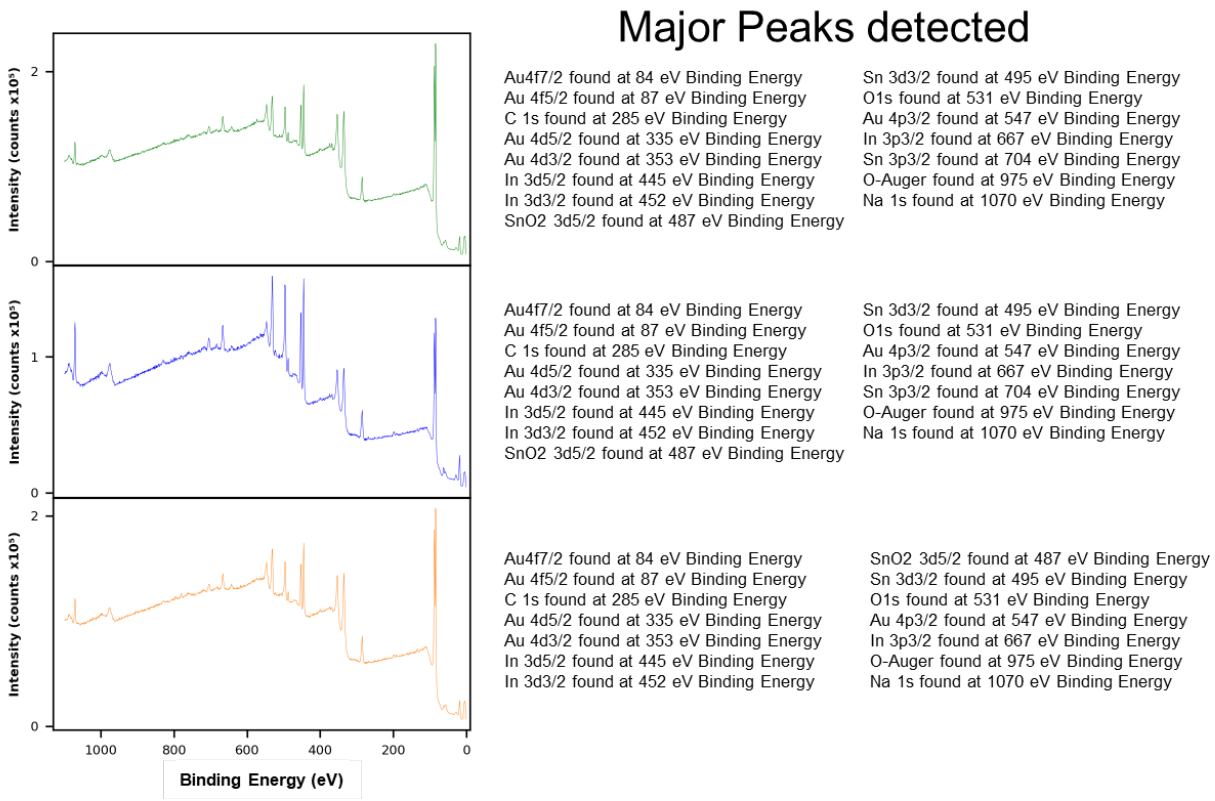

Figure S9. XPS survey scan of AuNPs treated with (**2**)AuCl (top), (**2**)AgCl (middle) or (**2**)CuCl (bottom). The spectra illustrate that the ITO substrate is not completely covered by the AuNPs since some peaks corresponding to indium oxide or tin oxide appear in each spectrum.

Theoretical Bonding Energy of (1)Au_{58} and (1)$AgAu_{57}$

Table S3. Bonding energy calculations for ligand **1** bound to an Au_{57} cluster through either an Au or an Ag adatom with either isopropyl groups in the down or up configuration relative to the surface.

	Au58	**Au57Ag**	**Difference**
isopropyl down	-94.9 kcal mol^{-1}	-81.7 kcal mol^{-1}	-13.2 kcal mol^{-1}
isopropyl up	-80.0 kcal mol^{-1}	-67.7 kcal mol^{-1}	-12.3 kcal mol^{-1}

ICP-OES Analysis of AuNPs Treated with Ligand 1 Metal Complexes

Figure S10. ICP-OES calibration curves for Au (left) and Ag (right).

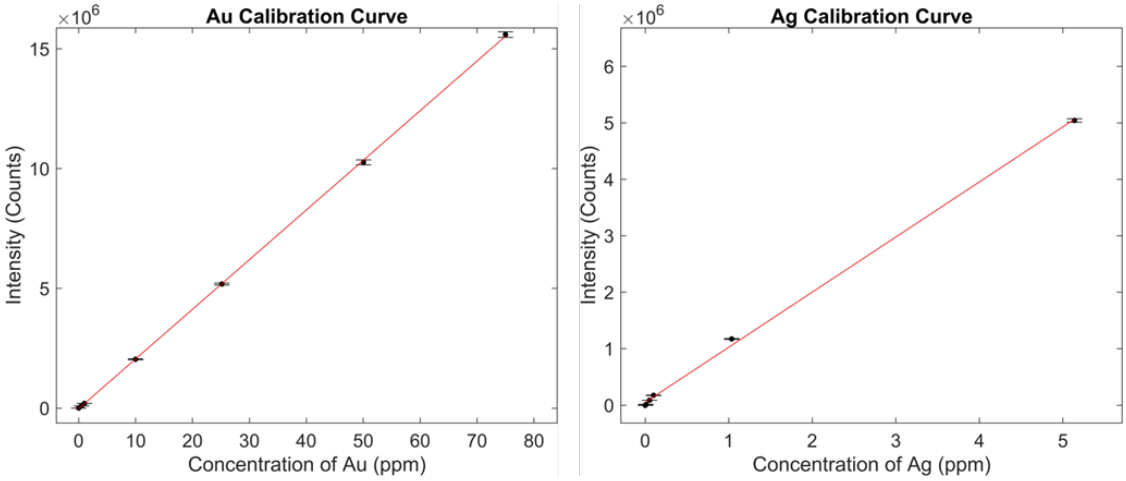

Table S4. The slope and intercept, standard deviation of the slope and intercept, and R^2 values for Au and Ag calibration curves are shown here.

Au Calibration Curve		
	slope	intercept
parameter	207413.06	-26696.62
std dev	887.27	34104.29
R^2	0.9999	
Ag Calibration Curve		
	slope	intercept
parameter	975763.36	51090.89
std dev	15164.94	32459.14
R^2	0.9990	

Table S5. Experimentally determined Au and Ag concentrations for AuNPs treated with (**1**)AuCl and (**1**)AgBr. The concentration of Ag in AuNPs treated with (**1**)AgBr is highlighted in green.

System	AuNPs + (**1**)AuCl	AuNPs + (**1**)AgCl
Au concentration	31.9 ± 0.4	18.6 ± 0.2
Ag concentration	-0.04 ± 0.03	0.25 ± 0.03
Percent Ag Incorporation	N/A	102 ± 14 %

ICP-OES Analysis of AuNPs Treated with Ligand 2 Metal Complexes

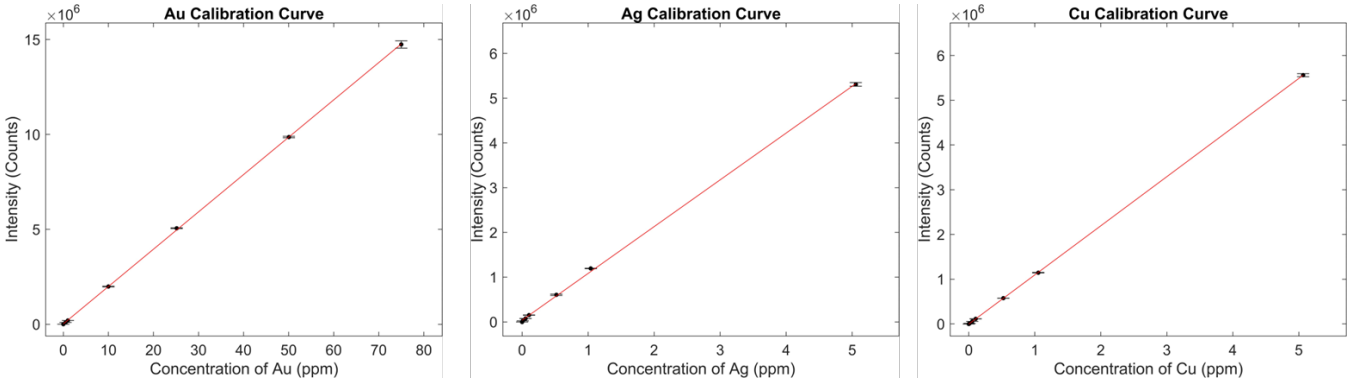

Figure S11. ICP-OES calibration curves for Au (left), Ag (middle), and Cu (right).

Table S6. The slope and intercept, standard deviation of the slope and intercept, and R^2 values for Au, Ag, and Cu calibration curves are shown here.

Au Calibration Curve		
	slope	intercept
parameter	196615.5	22183.32
std dev	617.26	21966.04
R^2	0.9999	
Ag Calibration Curve		
	slope	intercept
parameter	1045727	38055.66
std dev	9004.48	17656.98
R^2	0.9996	
Cu Calibration Curve		
	slope	intercept
parameter	1097815.94	-1868.87
std dev	994.29	1954.60
R^2	0.9999	

Table S7. Experimentally determined Au, Ag, and Cu concentrations for AuNPs treated with (**2**)AuCl, (**2**)AgCl, and (**2**)CuCl. The concentration of Ag or Cu in AuNP samples treated with (**2**)AgCl or (**2**)CuCl are highlighted in green.

System	AuNPs + (**2**)AuCl	AuNPs + (**2**)AgCl	AuNPs + (**2**)CuCl
Au concentration	24.6 ± 0.47	41.3 ± 0.2	30.1 ± 0.5
Ag concentration	-0.02 ± 0.02	0.12 ± 0.02	-0.03 ± 0.02
Cu concentration	0.004 ± 0.002	0.005 ± 0.002	0.015 ± 0.002
Percent Ag Incorporation	N/A	31 ± 5 %	N/A
Percent Cu Incorporation	N/A	N/A	10 ± 1 %

References

1. Ray L, Katiyar V, Barman S, Raihan MJ, Nanavati H, Shaikh MM, Ghosh P. Gold(I) N-heterocyclic carbene based initiators for bulk ring-opening polymerization of l-lactide. J Organomet Chem. 2007;692(20):4259-69. doi: 10.1016/j.jorganchem.2007.06.033.
2. Lee PC, Meisel D. Adsorption and surface-enhanced Raman of dyes on silver and gold sols. J Phys Chem-Us. 1982;86(17):3391-5. doi: 10.1021/j100214a025.
3. Velde Gt, Bickelhaupt FM, Baerends EJ, Guerra CF, Gisbergen SJAv, Snijders JG, Ziegler T. Chemistry with ADF. Journal of Computational Chemistry. 2001:931.
4. R. Rüger MF, T. Trnka, A. Yakovlev, E. van Lenthe, P. Philipsen, T. van Vuren, B. Klumpers, T. Soini. Theoretical Chemistry Amsterdam, The Netherlands: Vrije Universiteit; 2022.1. Available from: http://www.scm.com.
5. Becke AD. Density-functional exchange-energy approximation with correct asymtoticbehavior. Phys Rev A. 1988:3098–100.
6. Perdew JP. Density-functional approximation for the correlation energy of the inhomogeneous. Phys Rev B. 1986:8822–4.
7. Grimme S, Ehrlich S, Goerigk L. Effect of the Damping Function in Dispersion Corrected Density Functional Theory. Journal of Computational Chemistry. 2011:1457.
8. Lenthe Ev, Baerends EJ, Snijders JG. Relativistic regular two-component hamiltonians. J Chem Phys. 1993:4597–610.
9. Ghysels A, Neck DV, Waroquier M. Cartesian formulation of the Mobile Block Hessian Approach to vibrational analysis in partially optimized systems. Journal of Chemical Physics. 2007:164108.
10. Ghysels A, Neck DV, Speybroeck VV, Verstraelen T, Waroquier M. Vibrational Modes in partially optimized molecular systems. Journal of Chemical Physics. 2007:224102.
11. Jensen L, Zhao LL, Autschbach J, Schatz GC. Theory and method for calculating resonance Raman scattering from resonance polarizability derivatives. J Chem Phys. 2005:174110
12. The pymol molecular graphics system, version 1.2r3pre, schrödinger, llc. 2019.
13. Rost HL, Sachsenberg T, Aiche S, Bielow C, Weisser H, Aicheler F, Andreotti S, Ehrlich HC, Gutenbrunner P, Kenar E, Liang X, Nahnsen S, Nilse L, Pfeuffer J, Rosenberger G, Rurik M, Schmitt U, Veit J, Walzer M, Wojnar D, Wolski WE, Schilling O, Choudhary JS, Malmstrom L, Aebersold R, Reinert K, Kohlbacher O. OpenMS: a flexible open-source software platform for mass spectrometry data analysis. Nat Methods. 2016;13(9):741-8. doi: 10.1038/nmeth.3959.
14. Zhang Z-M, Chen S, Liang Y-Z. Baseline correction using adaptive iteratively reweighted penalized least squares. Analyst. 2010;135(5):1138-46. doi: 10.1039/b922045c.
15. Crudden CM, Horton JH, Ebralidze, II, Zenkina OV, McLean AB, Drevniok B, She Z, Kraatz HB, Mosey NJ, Seki T, Keske EC, Leake JD, Rousina-Webb A, Wu G. Ultra stable self-assembled monolayers of N-heterocyclic carbenes on gold. Nat Chem. 2014;6(5):409-14. doi: 10.1038/nchem.1891.
16. Major GH, Fairley N, Sherwood PMA, Linford MR, Terry J, Fernandez V, Artyushkova K. Practical guide for curve fitting in x-ray photoelectron spectroscopy. Journal of Vacuum Science & Technology A. 2020;38(6). doi: 10.1116/6.0000377.
17. Nakajima H. LG4X. Zenodo. 2021. doi: https://doi.org/10.5281/zenodo.3901523.
18. Newville M. OR, Nelson A., Ingargiola A., Stensitzki T., Allan D., et al. LMFIT: Non-Linear Least-Square Minimization and Curve-Fitting for Python2018;0.9.12. doi: 10.5281/zenodo.1699739.
19. Moulder JF, Chastain J. Handbook of x-ray photoelectron spectroscopy : a reference book of standard spectra for identification and interpretation of XPS data: Eden Prairie, Minn. : Physical Electronics Division, Perkin-Elmer Corp.; 1992.
20. Harris DC. Quantitative chemical analysis. 8th . ed: New York : W. H. Freeman and Co.; 2010.